J|A|C|S ARTICLES

Published on Web 02/18/2009

Shape- and Dimension-Controlled Single-Crystalline Silicon and SiGe Nanotubes: Toward Nanofluidic FET Devices

Moshit Ben Ishai and Fernando Patolsky*

School of Chemistry, The Raymond and Beverly Sackler Faculty of Exact Sciences, Tel Aviv University, Tel Aviv 69978, Israel

Received November 5, 2008; E-mail: fernando@post.tau.ac.il

Abstract: We report here on the formation of robust and entirely hollow single-crystalline silicon nanotubes, from various tubular to conical structures, with uniform and well-controlled inner diameter, ranging from as small as 1.5 up to 500 nm, and controllable wall thickness. Second, and most important, these nanotubes can be doped in situ with different concentrations of boron and phosphine to give p/n-type semiconductor nanotubes. Si_xGe_{1-x}-alloy nanotubes can also be prepared. This synthetic approach enables independent and precise control of diameter, wall thickness, shape, taper angle, crystallinity, and chemical/electrical characteristics of the nanotubular structures obtained. Notably, diameter and wall thickness of nearly any size can be obtained. This unique advantage allows the achievement of novel and perfectly controlled high-quality electronic materials and the tailoring of the tube properties to better fit many biological, chemical, and electrical applications. Electrical devices based on this new family of electrically active nanotubular building-block structures are also described with a view toward the future realization of nanofluidic FET devices.

Introduction

Since the first report on the synthesis of carbon nanotubes almost two decades ago,[1] much effort has been invested in the preparation of nanotubular materials.[2−4] Carbon nanotubes and nonporous membranes have been extensively used as templates for the subsequent preparation of nanotubular structures.[5,6] However, the nanotubes obtained are either porous, amorphous, or polycrystalline, and their shape and dimensions strongly depend on the characteristics of the available membranes and carbon nanotubes. Also, the synthesis of nonlayered GaN and SiO_2 nanotubes based on the use of core−shell nanowire templates has recently been published.[7,8] However, none of the publications mentioned have demonstrated the ability to synthesize nanotubular structures with uniform and controllable molecular-size inner diameters of less than 5 nm, with control over both the geometry and the chemical/electrical composition of the nanotube shell. Furthermore, the SiO_2 nanotubes obtained had amorphous structures. The growth of reproducible and controllable crystalline semiconductor nanotubes with uniform inner diameter and wall thickness, and controllable morphology, shape, and chemical composition, would be advantageous in potential nanoscale electronics, biochemical-sensing applications, and fluid-transport devices. In this regard, silicon nanotubes are of great importance. Silicon has been widely recognized as the most important material of the 20th century. This is largely due to its role as a fundamental component in integrated circuits and consequently in the microelectronics revolution. Although silicon nanotubes have stimulated great interest in nanomaterials as a result of their potential applications, they have generally been suggested theoretically,[9−12] because of the favorable formation of sp^3 hybridization of silicon in silicon nanotubes. Only recently have a few groups reported on the synthesis of silicon nanotubes,[13−19] each using a different growth process. However, the preparation of robust, crystalline silicon nanotubular structures is still a great challenge. It should be noted that none of the synthetic routes described has yet demonstrated the ability to synthesize robust, crystalline silicon

(1) Iijima, S. *Nature* **1991**, *354*, 56–58.
(2) Rapoport, L.; Fleischer, N.; Tenne, R. *J. Mater. Chem.* **2005**, *15*, 1782–1788.
(3) Tenne, R. *Prog. Inorg. Chem.* **2001**, *50*, 269–315.
(4) Tenne, R.; Zettle, A. K. *Carbon Nanotubes* **2001**, *80*, 81–112.
(5) Patzke, G. R.; Krumeich, F.; Nesper, R. *Angew. Chem., Int. Ed.* **2002**, *41*, 2446–2461.
(6) Martin, C. R. *Science* **1994**, *266*, 1961–1966.
(7) Goldberger, J.; He, R.; Zhang, Y.; Lee, S. W.; Yan, H.; Choi, H. J.; Yang, P. D. *Nature* **2003**, *422*, 599–602.
(8) Goldberger, J.; Fan, R.; Yang, P. D. *Acc. Chem. Res.* **2006**, *39*, 239–248.
(9) Fagan, S. B.; Baierle, R. J.; Mota, R.; da Silva, A. J. R.; Fazzio, A. *Phys. Rev. B* **2000**, *61*, 9994–9996.
(10) Seifert, G.; Kohler, T.; Urbassek, H. M.; Hernandez, E.; Frauen-Heim, T. *Phys. Rev. B* **2001**, *63*, 193409.
(11) Zhang, M.; Kan, Y. H.; Zang, Q. J.; Su, Z. M.; Wang, R. S. *Chem. Phys. Lett.* **2003**, *379*, 81–86.
(12) Bai, J.; Zeng, X. C.; Tankana, H.; Zeng, J. Y. *Proc. Natl. Acad. Sci. U.S.A.* **2004**, *101*, 2664–2668.
(13) Sha, J.; Niu, J.; Ma, X.; Xu, J.; Zhang, X.; Yang, Q.; Yang, D. *Adv. Mater.* **2002**, *14*, 1219–1221.
(14) Schmidt, O. G.; Eberl, K. *Nature* **2001**, *410*, 168.
(15) Jeong, S. Y.; Kim, J. Y.; Yang, H. D.; Yoon, B. N.; Choi, S.-H.; Kang, H. K.; Yang, C. W.; Lee, Y. H. *Adv. Mater.* **2003**, *15*, 1172–1176.
(16) Chen, Y. W.; Tang, Y. H.; Pei, L. Z.; Guo, C. *Adv. Mater.* **2005**, *17*, 564–567.
(17) Tang, Y. H.; Pei, L. Z.; Chen, Y. M.; Guo, C. *Phys. Rev. Lett.* **2005**, *95*, 116102.
(18) De Crescenzi, M.; Castrucci, P.; Scarcelli, M.; Diociauti, M.; Chaudhari, P. S.; Balasubramanian, C.; Bhave, T. M.; Bhoraskar, S. V. *Appl. Phys. Lett.* **2005**, *86*, 231901.
(19) Xie, M.; Wang, J. S.; Fan, Z. Y.; Lu, J. G.; Yap, Y. K. *Nanotechnology* **2008**, *19*, 1–4.

nanotubes with the aforementioned control over the properties of the nanotubes. This control is essential to the development of future nanoscale electronics and biochemical-sensing applications.

This article involves important innovative achievements. First, we demonstrate the formation of robust and entirely hollow single-crystalline silicon nanotubes, from various tubular to conical structures, with uniform and well-controlled inner diameter, ranging from as small as 1.5 up to 500 nm, and controllable wall thickness. Second, and most important, the chemical composition of the nanotubes can be readily modulated. Notably, diameter and wall thickness of nearly any size can be obtained. This unique advantage allows the achievement of high-quality electronic materials and the tailoring of the tube properties to better-fit many biological, chemical, and electrical devices applications.

Results and Discussion

In this article, we report on the use of sacrificial, "chemically soft" single-crystalline germanium-core nanowires as a base for the epitaxial growth of high-quality single-crystalline silicon nanotubes. Germanium nanowires were used as templates for the creation of core−shell heterostructures, in an ultrahigh-vacuum chemical vapor deposition (UHV-CVD) system. The use of germanium as a template offers the following advantages: (a) the core templates can be etched away by two alternative mechanisms. First, the germanium core can be selectively removed by wet-chemical etching; the other approach is the use of thermal oxidation of the germanium core. We would like to point out that neither etching method affects the integrity and the crystallinity of the resultant silicon nanotubes. The selective etching of germanium over silicon is of great importance for silicon technology. Different etchants with this property have been reported.[20,21] In this work, the etching process was carried out by a wet-chemical approach with the use of two etchants: (i) a mild H_2O_2 solution and[22] (ii) a stronger and faster-acting H_2O_2/NH_4OH etching solution. In both cases, germanium is oxidized by H_2O_2, and the resultant oxide is removed as a result of its high solubility in aqueous solution. The silicon walls of the nanotube remain intact and unetched as the oxidized silicon (SiO_2) is stable and insoluble in water, and so the etching process is terminated. (b) As the germanium core and the silicon shell both have diamond crystal structures with similar lattice constants (~4% difference), silicon can grow epitaxially on the germanium nanowires and form a single-crystalline sheath in an unannealed condition. Application of our method leads to the direct formation of crystalline silicon shells, without the requirement of a postgrowth annealing process, in contrast to previous reports on the growth of silicon shells on germanium nanowires.[23,24] Thus, by exploiting this epitaxial relationship, single-crystalline silicon nanotubes can be formed. Additionally, (c) the diameter of the germanium core can be reduced by postgrowth thermal oxidation to give ultrasmall nanotubes, and, alternatively, (d) ultralarge silicon nanotubes can be formed via a postgrowth enlargement process. (e) By altering the growth conditions, it is possible to form germanium templates of varying shapes and subsequently a variety of other hollow structures.

Crystalline germanium nanowire templates (as depicted in Figure 1A) were grown on (100) silicon wafers by the vapor−liquid−solid (VLS) mechanism, from gold nanoclusters, followed by conformally and epitaxially overcoating the cores with a silicon shell (and various reactants/dopants), with the use of a chemical vapor deposition system. The CVD approach coupled with VLS has been previously reported for the synthesis and study of germanium nanowires and Ge-core Si-shell nanowires[23−30] and has already demonstrated its ability to control the composition and the doping of the obtained nanostructures. Figure 1A shows a schematic outline of the procedure that generates silicon nanotubes by the nanowire-templating process. The first step involves the deposition of gold nanoclusters of the desired diameter on a silicon wafer, as seeds for the germanium-nanowire axial growth. The growth substrate was then placed inside a chemical vapor deposition system for the synthesis of the core (Ge)−shell (Si) nanowires. The diameter of the nanoparticles defined the diameter of the germanium core and the resultant inner diameter of the silicon nanotubes. The second step refers to the formation of the germanium-core template, with the use of germane (GeH_4) as a precursor and H_2 as a carrier gas in a well-known two-step CVD process.[28] The first step was carried out at 315 °C, to form nucleation sites for the following axial core-growth step, which occurred at a lower temperature (280 °C). The subsequent introduction of silane (SiH_4) into a mixture of H_2 and Ar as carrier gases, at a temperature of 450 °C, leads to the conformal and epitaxial formation of the silicon shell on top of the germanium-nanowire core. The resulting core−shell nanowire heterostructures can be sonicated off the growth substrate in a pentanol solution for the further germanium-core-etching step, leaving the crystalline silicon-shell nanotube intact. The etching step of the inner germanium-nanowire core is carried out in a solution of pentanol/30% hydrogen peroxide 3:1 v/v at 60 °C for 2 h, leaving the resultant nanotubes, which possess hydrophilic voids, unfilled by pentanol. After template removal, the color of the solution turns from dark brown to brownish. Alternatively, the core material can be etched away by the dry thermal oxidation of germanium in the presence of O_2 at temperatures above 350 °C, and the simultaneous vaporization of the germanium oxide, leading to the hollow nanostructures. Figure 1B shows a representative HRTEM image of high-quality single-crystalline germanium nanowires grown by CVD, with a diameter of about 20 nm (including a native-oxide sheath of about 2 nm). In agreement with previous studies[31] of VLS-grown nanowires, the diameter of the germanium nanowires correlates well with the diameter of the gold nanocluster: a sampling of 40 wires grown from 20 nm nanoclusters had a diameter of 20 ± 4 nm. HRTEM studies reveal that the as-prepared GeNWs have uniform structure and diameter along

(20) Krist, A. H.; Godbey, D. J.; Green, N. P. *Appl. Phys. Lett.* **1991**, *58*, 1899–1901.
(21) Carns, T. K.; Tanner, M. O.; Wang, K. L. *J. Electrochem. Soc.* **1995**, *142*, 1260–1266.
(22) Primak, W.; Kampwirt, R.; Dayal, Y. *J. Electrochem. Soc.* **1967**, *114*, 88–91.
(23) Sun, X. H.; Didychuk, C.; Sham, T. K.; Wong, N. B. *Nanotechnology* **2006**, *17*, 2925–2930.
(24) Lauhon, J. L.; Gudiksen, M. S.; Wang, D.; Lieber, C. M. *Nature* **2002**, *420*, 57–61.
(25) Dai, H.; Wang, D. *Angew. Chem., Int. Ed.* **2002**, *41*, 4783–4786.
(26) Hong, D.; Tu, R.; Zhang, L.; Dai, H. *Angew. Chem., Int. Ed.* **2005**, *44*, 2–5.
(27) Kim, C. J.; Yang, J. E.; Lee, H. S.; Jang, M. H.; Jo, M. H. *Appl. Phys. Lett.* **2007**, *91*, 3104–3109.
(28) Greytak, B. A.; Lauhon, L. J.; Gudiksen, M. S.; Lieber, C. M. *Appl. Phys. Lett.* **2004**, *84*, 4176–4178.
(29) Jin, C. B.; Yang, J. E.; Jo, M. H. *Appl. Phys. Lett.* **2006**, *88*, 1931–1934.
(30) Musin, R. N.; Wang, X. Q. *Phys. Rev. B* **2005**, *71*, 1553–1557.
(31) Cui, Y.; Lauhon, L. J.; Gudiksen, M. S.; Wang, J.; Lieber, C. M. *Appl. Phys. Lett.* **2001**, *78*, 2214–2216.

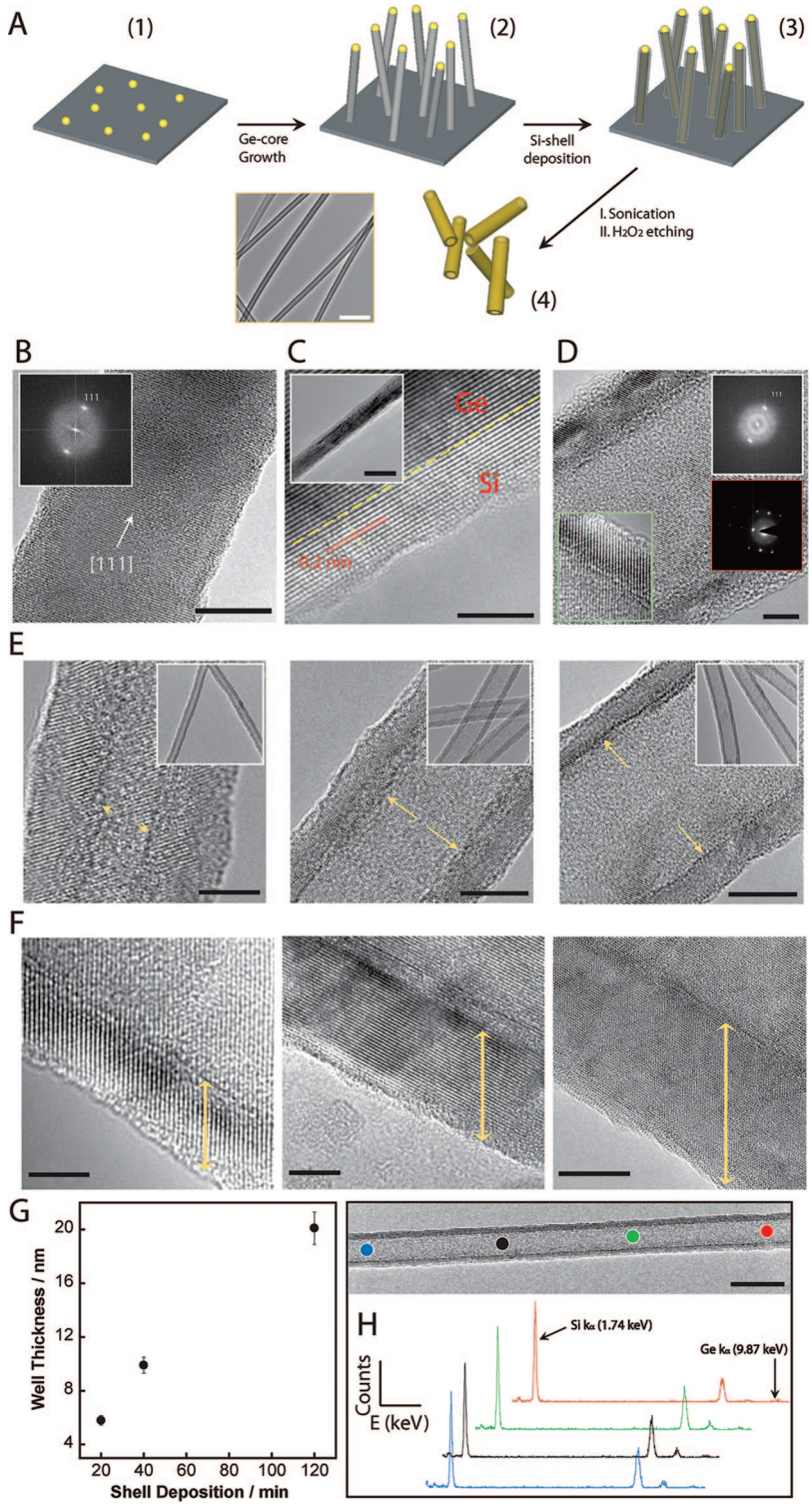

Figure 1. Synthesis and structural characterization of Si nanotubes. (A) Schematic illustration of the synthesis process of Si nanotubes. (1) Au nanoparticles dispersed on a Si substrate for (2) the formation of single-crystalline Ge nanowires at 280 °C, (3) Ge nanowires coated with Si at 450 °C, and (4) nanowires dispersed into pentanol and selectively etched by H_2O_2 to form Si nanotubes, as shown in the low-resolution TEM image. Scale bar is 400 nm. (B) Representative high-resolution TEM (HRTEM) images of a typical single-crystalline Ge nanowire and its fast Fourier transform (FFT) image (inset). (C) Typical HRTEM image of the junction between Ge core (dark) and Si sheath (light). The interplanar distance (0.20 nm) corresponds to (220) planes of Ge. Scale bar is 5 nm. The inset is a low-resolution TEM image of the corresponding sample. Scale bar is 50 nm. (D) HRTEM image of a typical single-crystalline Si nanotube. The lattice spacing corresponds to (111) planes of Si. Upper inset corresponds to the FFT of the same image. Bottom inset: HRTEM of the high-quality crystalline wall of the corresponding Si nanotube. Scale bar is 5 nm. Red boxed inset: Wide-field diffraction pattern of a representative silicon nanotube. (E) A series of representative HRTEM images of single-crystalline Si nanotubes with inner diameter of ca. 5 nm (left), 10 nm (middle), and 20 nm (right). Scale bars are 5 nm for left image, and 10 nm for both middle and right images. The arrows highlight the hollow-core region. Insets: Representative low-resolution TEM of the images shows that the nanotubes are straight with uniform diameter. (F) Set of typical HRTEM images taken from the edge of the nanotubes with uniform wall thickness of (1) ca. 5 nm, (2) 10 nm, and (3) 20 nm. Scale bars are 4, 5, and 10 nm, respectively. The arrows highlight the wall-thickness region. (G) Variation in the Si wall thickness as a function of the shell deposition time. (H) Representative energy-dispersive X-ray spectra recorded along the longitudinal axis of Si nanotube at different sites. The colored circles highlight the representative measured sites. Scale bar is 50 nm.

their entire length (more than 10 μm) with a lattice spacing of 0.33 nm. This corresponds to the *d*-spacing of the (111) crystal planes of germanium with a cubic structure, indicating that the germanium nanowires have preferential growth orientation in the [111] direction. The fast Fourier transform (FFT) of the HRTEM image (Figure 1B, inset), as well as XRD experiments on the as-grown Ge-nanowires substrate (data not shown), confirm that GeNWs are single-crystalline and grow with a diamond crystal structure and along the [111] direction.

The deposition of the silicon shell at 450 °C on top of the germanium nanowire surface results in single-crystalline Ge−Si core−shell structures. An HRTEM image of a typical Ge−Si core−shell structure (Figure 1C) exhibits a crystalline germanium core (dark) of about 20 nm and a continuous, uniform crystalline silicon shell (light) of about 5 nm along the entire length of the nanowire heterostructure. Further XRD experiments on the Ge/Si heterostructures reveal that the germanium cores and silicon shells are single crystals (data not shown). It is further noticed that the core/shell interface is compositionally sharp and no oxide layer was detected at the interface. A layer of amorphous SiO_2 about 1 nm thick covers the outer surface of the nanowires. This layer formed probably when the nanowires were exposed to ambient environment, similar to the oxide sheathing of silicon nanowires previously reported.[32] Both the core and the shell regions have lattice spacing of 0.20 nm, which is in excellent agreement with the (220) planes of the known diamond crystal structure of germanium. This observation indicates a continuous epitaxial layer of silicon on the germanium core without the requirement of a postgrowth annealing process.[23,24] In addition, energy-dispersive X-ray spectroscopy (EDX) measurements confirm the existence of the elements germanium and silicon at a nearly uniform atomic ratio of 1.04:1.00. Selective etching of the germanium cores successfully transformed the Ge−Si core−shell nanowires into crystalline silicon nanotubes. A representative HRTEM micrograph of a typical silicon nanotube (Figure 1D) shows that the obtained nanotubes have a uniform and high-quality single-crystalline structure along their entire length (more than tens of micrometers) and further confirms that these nanotubes are entirely hollow with no defects along their length due to the strain introduced on the thin-wall structures. In addition, wide-field selected-area diffraction (SAED) measurements, Figure 1D red boxed inset and Supporting Information Figure S1, further confirm that the silicon nanotubes are indeed single crystalline. Also, XRD experiments on the silicon nanotubes confirm the tubes are single crystals regardless of the thickness of the silicon shell (data not shown). The image contrast clearly shows a uniform hollow core of about 20 nm and a uniform wall thickness of about 5 nm, which are equal to the original germanium core diameter and silicon shell thickness, respectively. The lattice-plane spacing obtained for a typical nanotube, 0.314 nm, agrees well with the interplanar distance of silicon with a cubic structure. In contrast with this, the measured spacing of the crystallographic planes in core−shell nanowires (Figure 1C) matched the interplanar distance of germanium. This observation, which is consistent with all of the results of our studies on nanotubes, indicates that, after the etching process, the silicon nanotubes have relaxed to their equilibrium lattice spacing. The corresponding two-dimensional Fourier transform (2DFT) of the lattice-resolved image (upper inset of Figure 1D) can be indexed to the diamond structure of silicon with a [111] growth direction. Further confirmation of this assignment was carried out by EDX analysis. The representative EDX spectra (Figure 1G, left), which are common to all of the hollow nanostructures in this work, reveal a very small residue of germanium, less than 1%, and a well-correlated silicon signal along the longitudinal axis of the nanotubes. This result indicates successful preparation of the silicon nanotubes. Because the diameter of the gold eutectic-liquid droplet is the primary factor in controlling the nanowire diameter of the VLS growth,[33−35] and thus the inner diameter of the resultant nanotubes, it is possible to form nanotubes with different inner diameters simply by changing the size of the nanocluster. Figure 1E shows a set of representative HRTEM micrographs of the as-prepared single-crystalline silicon nanotubes with different inner diameters. The contrast of the images clearly shows hollow cores of about 5, 10, and 20 nm, which are nearly the same as the initial sizes of the gold nanocatalysts. These nanotubes are straight and smooth, with uniform diameter and wall thickness of about 5 nm along their longitudinal axis and with excellent crystallinity. The lattice spacing obtained for each typical nanotube and the corresponding FFTs (see Supporting Information, Figure S2A, S2B, and S2C) agree well with the interplanar distance of silicon with a diamond-like crystal structure. It is also feasible to control the wall thickness of the nanotubes by adjusting the deposition time of the silicon shell. We have studied the effect on the wall thickness of three different shell-deposition times. This effect can be seen in Figure 1F, which shows a series of HRTEM images of single-crystalline silicon nanotubes, with uniform wall thickness of about 5, 10, and 20 nm corresponding to 20, 40, and 120 min of shell-deposition time. Figure 1G, right image, clearly shows the monotonic increase of the shell thickness as a function of the shell-deposition time. Furthermore, the corresponding FFTs of the HRTEM images show that the nanotubes obtained have the cubic diamond-crystal structure of silicon (see Supporting Information, Figure S3A, S3B, and S3C).

With further optimization and control of the core-template diameter, we have successfully synthesized nanotubes with ultrasmall inner diameters, down to about 1.5 nm, and ultralarge diameters of 100 and about 400 nm. It is worth pointing out that the VLS growth of germanium nanowires from large gold seed particles ($d \geq 50$ nm) tends to produce germanium nanowires in low yields at low growth temperatures, or to overproduce nanowires at high temperatures, as a result of splitting of the gold seeds.[26] On the other hand, small gold seeds ($d \leq 5$ nm) grow nanowires of diameters larger than those of the initial particles, a result of simultaneous axial and radial growth. To overcome these limitations, two strategies have been developed in this work. The first involves the enlargement of the as-grown germanium core leading to the synthesis of nanotubes with ultralarge inner diameters. Figure 2A schematically describes the synthesis of nanotubes based on this approach. The second step is the core-enlargement process. This step involves conformal deposition of a germanium shell on top of the original germanium core (20 nm). Note that the growth of the germanium shell is carried out at a higher

(32) Hofmann, S.; Ducati, C.; Neill, R. J.; Piscaec, S.; Ferrari, A. C.; Geng, J.; Dunin-Borkowski, R. E.; Robertson, J. *J. Appl. Phys.* **2003**, *94*, 6005–6012.

(33) Xia, Y.; Yang, P.; Sun, Y.; Wu, Y.; Mayers, B.; Gates, B.; Yin, Y.; Kim, F.; Yan, H. *Adv. Mater.* **2003**, *15*, 353–389.

(34) Wanger, S. In *Whisker Technology*; Levit, A. P., Ed.; Wiley Interscience: New York, 1970; pp 47−119.

(35) Greytak, A. B.; Lauhon, L. J.; Gudiksen, M. S.; Lieber, C. M. *Appl. Phys. Lett.* **2004**, *84*, 4176–4178.

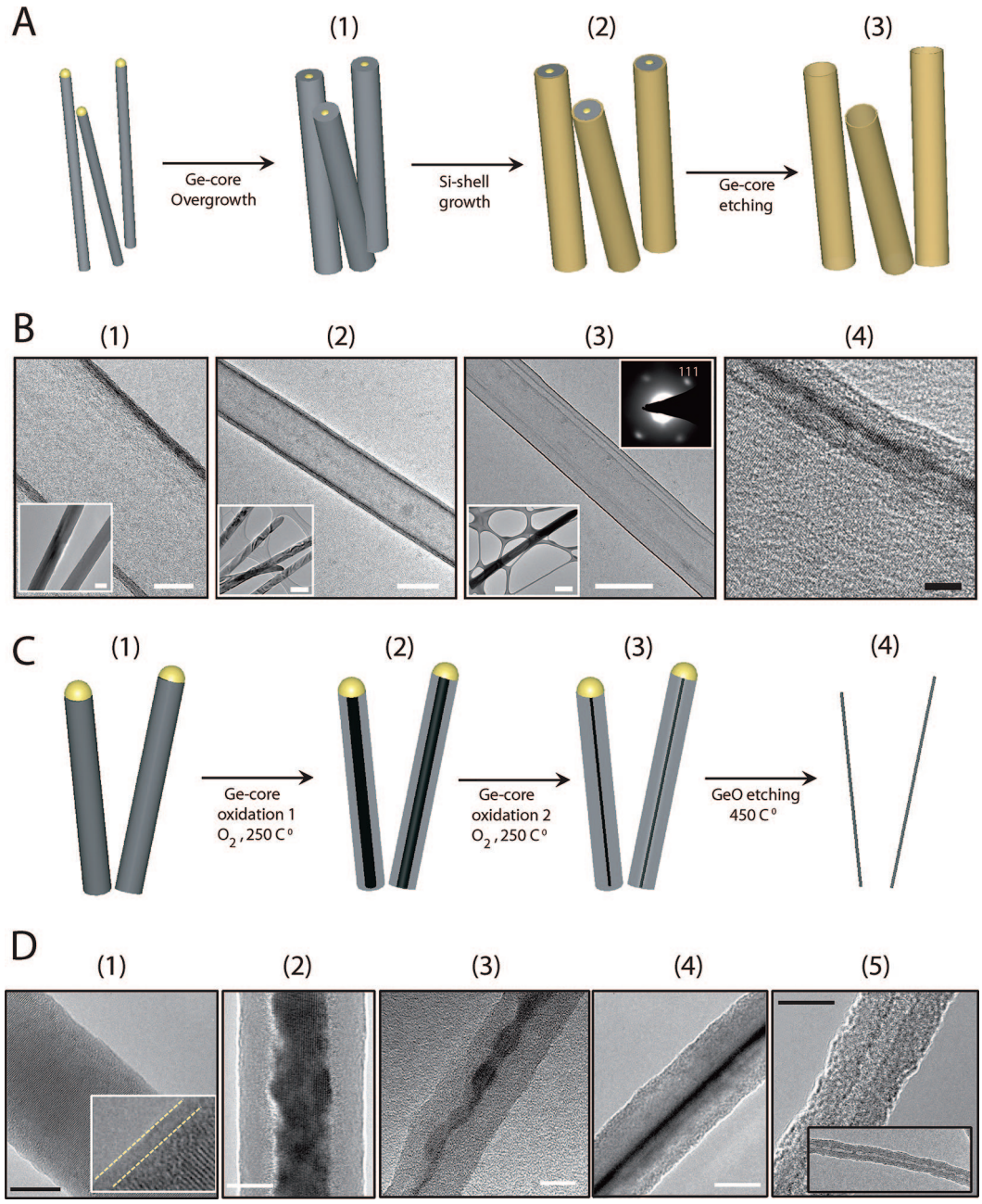

Figure 2. Synthesis and characterization of ultralarge and ultrasmall silicon nanotubes. (A) A schematic drawing depicting the postgrowth enlargement process. (1) Ge nanowires are coated with Ge shell for different deposition times, (2) epitaxially coating with Si, and (3) nanowires dispersed into pentanol and selectively etched by H_2O_2 to form Si nanotubes. (B) Series of low-resolution TEM images of a typical single-crystalline Si nanotube with uniform inner diameter of (1) 60 nm, (2) 100 nm, and (3) 400 nm. Scale bars are 20, 50, and 100 nm, respectively. The bottom insets are representative low-resolution TEM images of the corresponding Ge core-template after the enlargement process. Scale bars are 300 nm, 400 nm, and 1 μm, respectively. The upper inset in image 3 corresponds to a representative electron-diffraction pattern of the nanotubes. (4) HRTEM image of sample 3. Scale bar is 5 nm. (C) Schematic illustration of the postgrowth thermal-oxidation process. (1) Thermal etching of the native-oxide (GeO_2) sheath covers the Ge core surface. (2, 3) Thermal oxidation of the Ge core for different lengths of time. (4) Thermal etching of the GeO_2 layer results in smaller Ge cores. (D) (1) HRTEM image of a Ge core with a diameter of ca. 20 nm. The dashed lines highlight the native oxide (GeO_2) of 1−2 nm. Images 2, 3, and 4 show a series of low-resolution TEM images of Ge−GeO_2 core−sheath at different oxidation times. Scale bars are 10 nm for images 1, 2, and 3, and 20 nm for image 4. (5) HRTEM image of a typical Si nanotube with a minimum inner diameter of ca. 2.2 nm. Scale bar is 11 nm. The inset shows a low magnification of Si NTs with inner diameter of 1.5 nm.

temperature (360 °C) to promote the radial growth. By varying the deposition time of the germanium shell, it is possible to enlarge the original core diameter considerably while keeping intact the crystallinity of the germanium core. The deposition of the silicon shell on top of the "broadened" germanium nanowires (third step), followed by the selective removal of the germanium core (step 4), leads successfully to crystalline silicon nanotubes with larger inner diameters. Low-resolution TEM studies (Figure 2B) of nanotubes prepared in this way show nanotubes with uniform inner diameters of about 60 nm (image 1), 100 nm (image 2), and 400 nm (image 3), and uniform contrast along their entire length (tens of micrometers), which are properties indicative of crystalline structures. These diameters are consistent with the diameters of the germanium-core templates after the enlargement process (lower insets of Figure 2B). Note that in all cases the enlargement process was

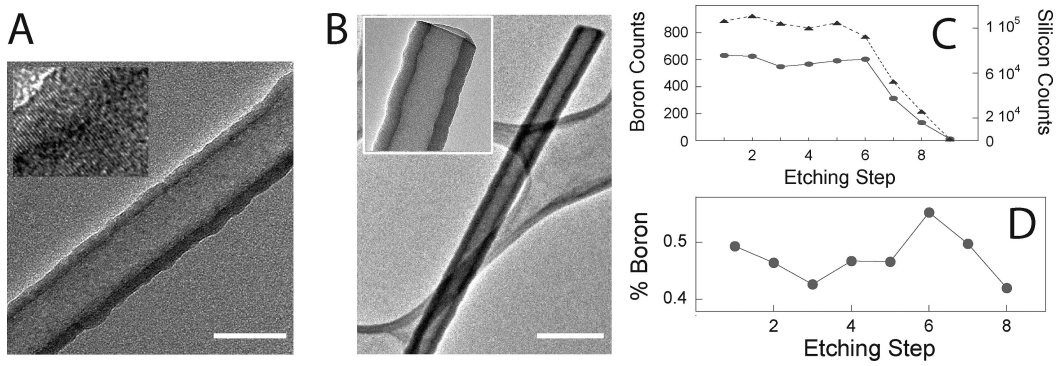

Figure 3. Synthesis and characterization of nanotubes with various compositions: GeSi-alloy nanotubes and p-type doped nanotubes. (A) Low-resolution TEM image of a typical $Si_{0.94}Ge_{0.06}$ alloy nanotube. Scale bar is 50 nm. Inset: HRTEM of the nanotube edge, shows high-quality single-crystalline structure, with lattice spacing of 0.318 nm. (B) Representative low-resolution TEM image of in situ p-type doped Si nanotube. Scale bar is 200 nm. The inset shows high magnification of the open-ended nanotube. (C,D) Compositional depth profile of the nanotubes, probed by time-of-flight secondary-ion mass spectroscopy (TOF-SIMS) measurement.

performed on the original 20 nm germanium nanowires. A typical HRTEM of the as-prepared silicon nanotubes (Figure 2B, image 4) indicates that the nanotubes are single crystalline with the same crystal orientation along the entire length of the nanotube and with a uniform and smooth wall thickness of about 5 nm. In addition, the selected-area electron-diffraction (SAED) pattern (Figure 2B, inset, image 3), taken from a typical nanotube, confirms the fact that the resultant nanotubes have the diamond cubic structure of silicon with [111] growth direction.

The second approach involves the thermal oxidation of the postgrowth core. This makes it possible to prepare nanotubes with inner diameters of less than 1.5 nm. Figure 2C shows a schematic outline of the steps required to reduce the diameter of the as-prepared germanium-core templates. Systematic variation of the thermal-oxidation time over the range of 1−3 h, at 250 °C and 1 torr O_2, enables us to control reproducibly and considerably reduce the diameter of the germanium-nanowire templates obtained by the conventional synthetic procedure (Figure 2C, (3) and (4)). It should be emphasized that the first step, which involves vaporization at 450 °C of the native-oxide sheath (GeO_2) of about 1 nm thickness (dashed lines in the inset of Figure 2D, (1)), is a crucial step. Without this step, the germanium core cannot be oxidized even at high temperatures. Referring to the low-resolution TEM images in Figure 2D of germanium nanowires before oxidation (Figure 2D, (1)) and after it (Figure 2D, (2), (3), (4)), one can clearly see the distinct boundary between the amorphous germanium-oxide layer (light region) and the germanium core (dark region), and the sharp reduction in the core diameter, from about 20 nm for the original core template (Figure 2D, (1)) to about 10 nm (Figure 2D, (2)), about 4 nm (Figure 2D, (3)), and about 1.5 nm (Figure 2D, (4)), along with the monotonic increase of the oxide-sheath thickness, which was also revealed by the low-resolution TEM.

Finally, vaporization and removal of the oxide layer at 450 °C, followed by the growth of a conformal silicon shell and the selective etching of the germanium core, lead to the formation of nanotubes of inner diameter significantly smaller than that of the initial core-template. Figure 2D, (5) shows an HRTEM image of a typical silicon nanotube with a minimum internal diameter of about 1.5 nm, which was formed after thermal oxidation. The hollow interior of the small-diameter nanotube can be clearly seen. The roughness of the walls of these tubes is the result of the germanium-core oxidation prior to the deposition of the silicon shell, as can be clearly seen in Figure 2D. To the best of our knowledge, this is the first report of crystalline silicon nanotubes of such ultrasmall diameter. These preliminary results show that it is possible to synthesize nanotubular structures with ultrasmall inner diameters of less than 2 nm. Further experiments are being performed to improve the oxidation conditions of the nanowire templates in terms of diameter and oxidation rate.

A unique advantage of our synthetic approach is that it provides us with rational and precise control over the chemical composition of the silicon nanotubes. By subsequent introduction of dopants and other reactants, nanotubes of different composition can be formed. Specifically, single-crystalline Si_xGe_{1-x} alloy nanotubes (Figure 3A) and p-type silicon nanotubes (Figure 3B) were synthesized on the basis of our template approach, with the use of germane (GeH_4) and diborane (B_2H_6), respectively. These were fed into the CVD system simultaneously with silane (SiH_4) during the shell-growth step. The ability to synthesize p/n-type nanowires and Si_xGe_{1-x} alloy nanowires via the CVD-VLS method has already been demonstrated;[24,27,28] however, to the best of our knowledge, this work is the first to report the synthesis of Si_xGe_{1-x} alloy and doped silicon nanotubes. Si_xGe_{1-x} alloy nanotubes were identified as $Si_{0.94}Ge_{0.06}$ by EDX measurements with the use of a k factor of Si K_α and Ge K_α radiation in the EDX spectra. The Si:Ge composition, which varies by not more than 0.5% along the length of the nanotube, suggests appropriate alloying of silicon and germanium. We also confirmed that $Si_{0.94}$:$Ge_{0.06}$ alloy nanotubes are single crystalline with the same crystal orientation along the entire nanotube length as in Figure 2J, inset. The observed lattice spacing (0.318 nm) corresponds to the d-spacing of the (111) crystal planes of silicon with a cubic structure and [111] growth direction. Si_xGe_{1-x} alloy nanotubes of different Si:Ge compositional ratio can be obtained with the use of the proposed approach, because concentrations of germanium lower than 60% lead to nanotube walls stable in the H_2O_2 etching solution. Higher percentages of germanium lead to nanotube walls unstable to the etching step of the germanium core. The presence of silicon in the alloy at concentrations higher than 40% inhibits the etching of the SiGe alloy.[36] Future studies will be performed on SiGe alloy nanotubes to expand the Si−Ge

(36) Bircumshaw, B. L.; Wasilik, M. L.; Kim, E. B. Y. R.; Takeuchi, H.; Low, C. W.; Liu, G.; Pisano, A. P.; King, T.-J.; Howe, R. T. *Technical Digest*; IEEE, 17th International Conference on Micro Electro Mechanical Systems, 2004; p 514.

composition spectrum and to electrically characterize the obtained nanotubes.

For p-type silicon nanotubes, we quantitatively determined the relative boron composition using time-of-flight secondary-ion mass spectroscopy (TOF-SIMS) analysis combined with a sputtering etching process. A compositional depth profile, which was carried out on the nanotubes, as representatively shown in Figure 3C and D, reveals the boron composition of the silicon-nanotube wall. The B/Si atomic ratio, which was measured sequentially after multiple etching steps of the nanotubes, was ~1/200. Subsequent introduction of diborane during the growth step of the silicon shell greatly influenced the wall thickness of the obtained nanotubes. Low-resolution TEM performed on the p-type nanotubes (Figure 3B) shows that the wall thickness of the nanotubes was about 20 nm, as compared to about 10 nm for the pristine silicon nanotubes (Figure 1F, middle) for an identical shell-growth duration of 40 min. This is in agreement with previous reports on the growth of a silicon shell on top of germanium nanowires.[37] By changing the partial pressure of the reactants, it is possible to form p/n-type silicon nanotubes and Si_xGe_{1-x} nanotubes with different doping density and Si:Ge ratio.

The shape of semiconductors at the nanoscale is another factor that influences their properties, and thus the shape-controlled growth of semiconductors can find unique applications in electronics and photonics. Our approach can be also extended to produce a variety of other hollow forms, such as "hollow cones" (Figure 4A). Nanocones have been reported for carbon, but the intrinsic fullerene lattice strongly limited the taper angles achievable.[38]

Figure 4A schematically illustrates the experimental procedure used to fabricate conical silicon nanotubular structures. The same steps described previously were used to produce the hollow cones, except for the nanowire-template growth. Here, the formation of nanowire templates was carried out at higher temperatures to produce a cone-like shape as a result of simultaneous axial and conformal radial growth. The fabrication of germanium-cone nanowires with different taper angles by a CVD-VLS method has been already demonstrated and studied.[28,39] To form conical nanotubular structures with different taper angles, a series of nanowire templates was grown at temperatures of 340, 360, and 380 °C. Figure 4B shows a series of scanning electron microscopy (SEM) images of germanium nanostructures whose shape can be controllably tuned from nanowires, which were grown at 280 °C, to nanocones with various taper angles, at higher growth temperature, up to 380 °C. The relationship between the taper angle and the growth temperature is depicted in Figure 4B, (5). Figure 4B, (5) is constructed on the basis of statistical distributions of taper angles measured over 10 germanium-cone nanowires at each growth temperature (340, 360, and 380 °C). We see that the taper angle strongly depends on the growth temperature, and it increases by a factor of 2 as the temperature is raised from 340 to 380 °C. The conical nanowires that were grown at 380 °C were coated with a 5 nm-thick silicon shell. Both low- and high-resolution TEM images were used to characterize the shape, shell thickness, and crystallinity of the conical nanowires. Figure 4C, (1) shows a representative low-resolution image of a conical germanium nanowire grown at 360 °C. A high-resolution TEM image of a typical Ge−Si core−shell conical nanowire shown in Figure 4C, (2) reveals the high-quality single-crystalline core−sheath structure and confirms the epitaxial growth of the capping shell along the entire length of the conical template structure. The lattice spacing of both the shell and the core (0.33 nm) corresponds to the *d*-spacing of (111) crystal planes of germanium with cubic structures. This observation was confirmed by the FFT of the TEM image (inset of Figure 4C, (2)). Selective extraction of the germanium core from the core−shell nanocones results in the formation of hollow silicon cones, as shown in Figure 4C, (3). The nanotubular structure is complementary to the morphology of the germanium template with the interior void determined by the dimensions of the core template, which grows at 380 °C. A lattice-resolved image of a typical conical nanotube and its FFT image indicate that the resultant nanotubes have a cubic diamond crystal structure of silicon with [111] growth direction.

Our approach exhibits a further degree of controllability because both the shape and the taper angle can be controlled by adjusting the growth variables. In addition, we have developed a synthetic procedure for creating funnel-like nanotubular structures (Figure 4D). Figure 4D schematically outlines the major steps required to do this. Here, the fabrication of the germanium template involves two steps. It will be noted that the nanotubes consist of two structures, cone and wire, and each step leads to the formation of one of the nanostructures. At first, the temperature was set at 360 °C to form the cone, and then with continued flow of germanium, the temperature was gradually lowered to 280 °C to initiate wire growth. To further continue the wire growth, the temperature was maintained at 280 °C. A low-resolution TEM image (upper image of Figure 4E, (1)) shows a typical funnel-like nanowire template. The junction point between the cone and the wire, and the wire region, are marked and magnified (lower images of Figure 4E, (1)). The funnel-like nanowire templates were then transformed into nanotubular structures with uniform, highly crystalline sheath and smooth surface. Figure 4E, (2) shows a low-resolution TEM image of a representative hybrid nanotube. The nanotubes obtained have morphology complementary to that of the germanium template that grows at 340 °C. Detailed studies with the use of high-resolution TEM (Figure 4E, (3)) verified that the resulting nanotubular structures are high-quality single-crystalline silicon and the reciprocal lattice peaks obtained from the FFT (Figure 4E, (3), inset) can be indexed to the cubic structure of silicon with [111] growth direction.

In addition, we have extended our research into the chemical functionalization of the nanotubes, which is a crucial step to many future applications, including chemical separations (selective filtering), selective transport, and sensing of chemical and biological molecules. Pristine silicon nanotubes are insoluble in most solvents and show a strong tendency to form aggregates. To improve their solubility, silicon nanotubes were chemically modified by the covalent binding of silane molecules containing different functional groups to their outer surface. Figure 5A schematically describes the functionalization procedure used for the dispersion of silicon nanotubes (Figure 5B). All modifications were carried out on the surface of the core−shell nanowires. This allows us to modify the external surface of the subsequent nanotubes without affecting their inner surface. The outer surface of the silicon nanowires is terminated by silanol groups (SiOH), which are employed as anchoring sites for silane

(37) Briand, D.; Sarret, M.; Kis-Son, K.; Mohammed-Brahim, T.; Duverneuil, P. *Sci. Technol.* **1999**, *14*, 173–180.
(38) Krishnan, A.; Dujardin, E.; Treacy, M. M. J.; Hugdahl, J.; Lynum, S.; Ebbesen, T. W. *Nature* **1997**, *388*, 451–454.
(39) Dailey, J. W.; Taraci, J.; Clement, T.; Smith, J. D.; Drucker, J.; Picraux, S. T. *J. Appl. Phys.* **2004**, *96*, 7556–7567.

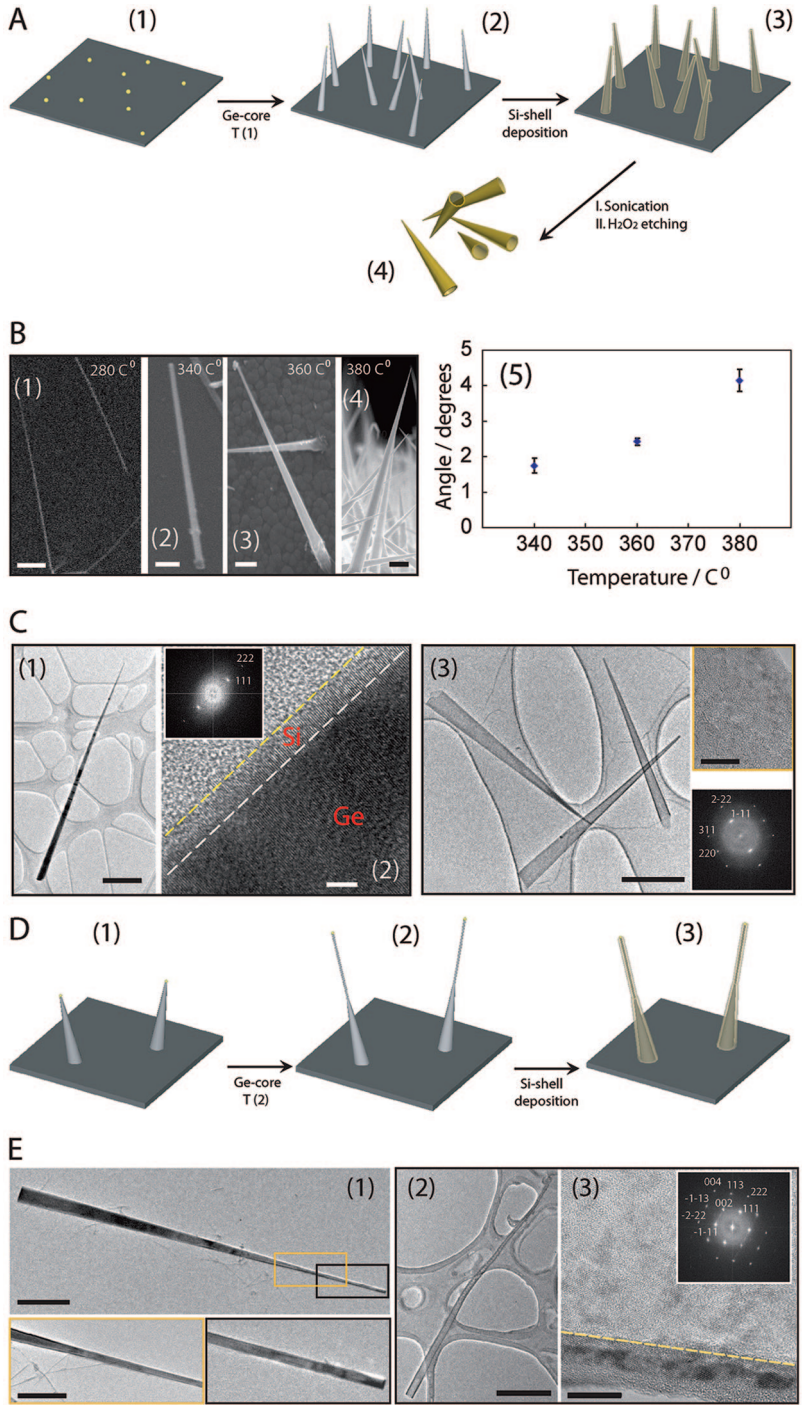

Figure 4. Synthesis and structural characterization of conical and funnel-like nanotubular structures. (A) Schematic illustration of the experimental procedure for synthesis of hollow cones. (1) Deposition of Au nanoparticles, and (2) growth of Ge-cone nanowire at 360 °C, which were (3) epitaxially coated with Si shell at 450 °C and (4) dispersed into pentanol and chemically etched with H_2O_2 to form the Si conical nanotubular structure. (B) A set of representative scanning electron microscopy (SEM) images of the as-synthesized Ge-cone templates. The shape varies from (1) wire at 280 °C, with uniform diameter of 20 nm along the entire length, to conical shape with various taper angles. Scale bars are 300 nm, 150 nm, 300 nm, and 1 μm. (5) Variation in the taper angle of the Ge cone as a function of temperature. Scale bars are 300, 150, and 300 nm, respectively. (C) Structural characterization of the Ge−Si core−shell conical nanowire and the resultant Si conical nanotubular structure. (1) Low-resolution TEM image of a typical Ge−Si core−shell cone grown at 380 °C. Scale bar is 1 μm. (2) HRTEM image of the cone edge and its FFT (inset) showing that both Ge core (dark) and Si shell (bright) grow with a diamond crystal structure of Ge and along [111] growth direction. Scale bar is 5 nm. (3) Low-resolution TEM image of the conical nanotubular structure. Insets: Lattice-resolved TEM image of nanotubes and its FFT. Scale bars are 1.5 μm and 10 nm, respectively. (D) Schematic illustration of the formation of Ge−Si core−sheath funnel-like nanowire. (1) Ge cones grow at a temperature of 360 °C, and then (2) under continued flow of GeH_4, the temperature was gradually lowered to 280 °C to initiate growth of the wires and then maintained at 280 °C to continue growth of the wires to form funnel-like nanowires, which were (3) covered with a Si shell to give Ge−Si core−shell funnel-like nanowires. (E) (1) Low-resolution TEM image of a typical nanowire with a funnel-like shape. The junction point between the wire and the cone, and the region of wire growth from within the yellow rectangle and dark rectangle, are expanded to the bottom. Scale bars are 600 and 300 nm, respectively. (2) Low-resolution TEM of the funnel-like nanotube. Scale bar is 500 nm. (3) HRTEM of the sample in image (2) and its FFT. Scale bar is 10 nm.

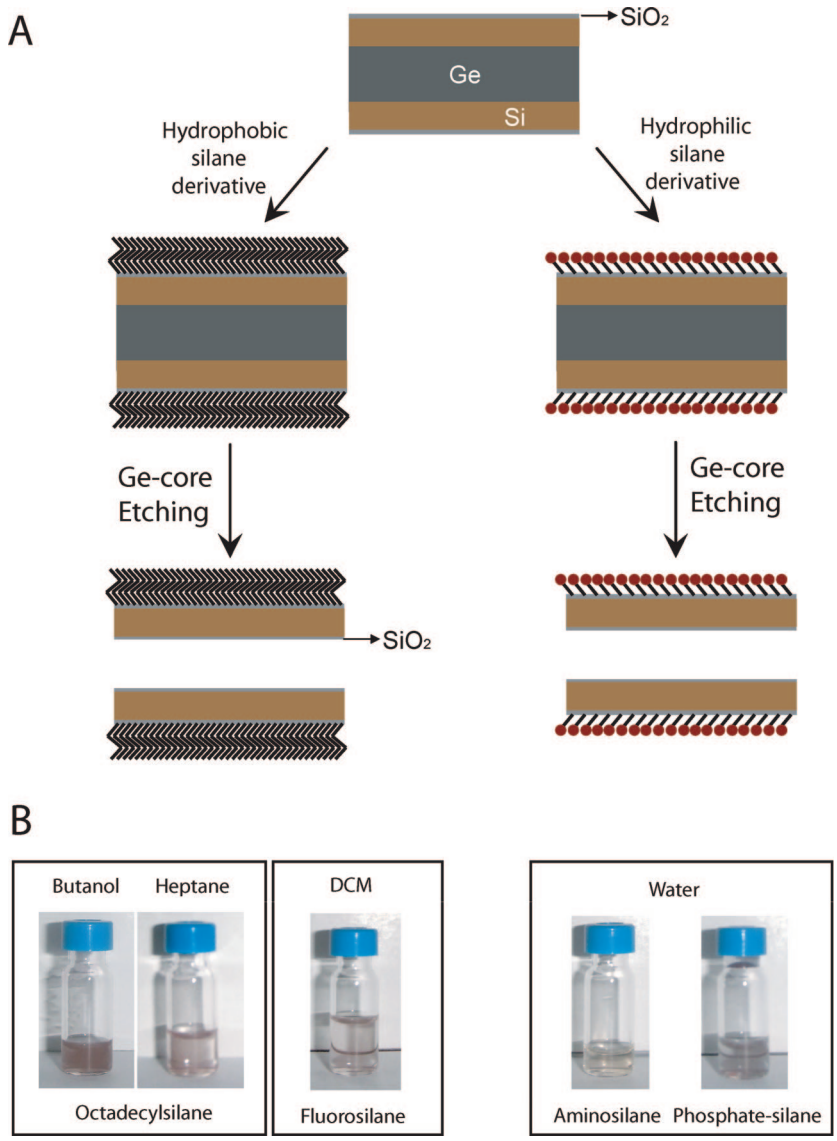

Figure 5. (A) Schematics of the approach used for the functionalization of the Si nanotubes by various silane derivatives. (B) Dispersions of the resultant functionalized Si nanotubes in various solvents.

molecules to form Si−O−Si covalent bonds. Silanes are known to facilitate the solubility of nanowires and nanotubes in different solvents.[40−42] Surface modification with silanes can be carried out in the gas phase or by wet chemistry. In the present study, we used the latter approach. The modification process is begun with the direct attachment of silane derivatives with different functional groups to the silicon shell of the nanowire template. This is done by incubating the growth substrate in a solution of the silane derivative for 2 h. The functionalized nanowire substrate is then rinsed with the appropriate solvents and cured for 10 min in an oven at 110 °C. The next step involves removal of the nanowires from the SiO_2 substrate by sonication and further etching of the core material. Next, the functionalized silicon nanotubes are centrifuged, washed, and dispersed into liquid suspensions (common organic solvents and water). This results in either a hydrophobic or a hydrophilic exterior surface of the nanotube. The interior, which was left unfunctionalized, is a hydrophilic void and can be readily modified in later steps. Figure 5B illustrates representative results of the functionalized Si-nanotube dispersions. Covalent linking of aminosilane or phosphate−silane to the surface of silicon nanotubes produces tubes readily soluble in water. Functionalized silicon nanotubes soluble in organic solvents include nanotubes prepared with fluorosilane and octadecylsilane.

The integration of nanotubular building blocks into electrical devices is of critical importance for most required applications. Thus, we have fabricated FET devices from our p-doped silicon nanotubes and carried out electrical-transport measurements to evaluate their performance. The assessment of the electrical properties of nanotubes is a key step in the evaluation of their suitability for electrical applications. For the fabrication of our p-type FETs, a liquid suspension of silicon nanotubes with inner diameter of about 20 nm and wall thickness of 4 nm was first dispersed on a highly doped silicon substrate with a 600 nm-thick silicon oxide (SiO_2) dielectric layer. This was followed by the formation of Ni/Au source-drain electrodes/contacts by e-beam lithography. Figure 6A shows an HRSEM image of a typical device consisting of an individual silicon nanotube with

(40) Sagiv, J. *J. Am. Chem. Soc.* **1980**, *102*, 92–98.
(41) Duchet, J.; Chabert, B.; Chapel, J. P.; Gerard, J. F.; Chovelon, J. M.; Jafferzic-Renault, N. *Langmuir* **1997**, *13*, 2271–2276.
(42) Pershan, P. S.; Axe, J. D. *J. Am. Chem. Soc.* **1989**, *111*, 5852–5856.

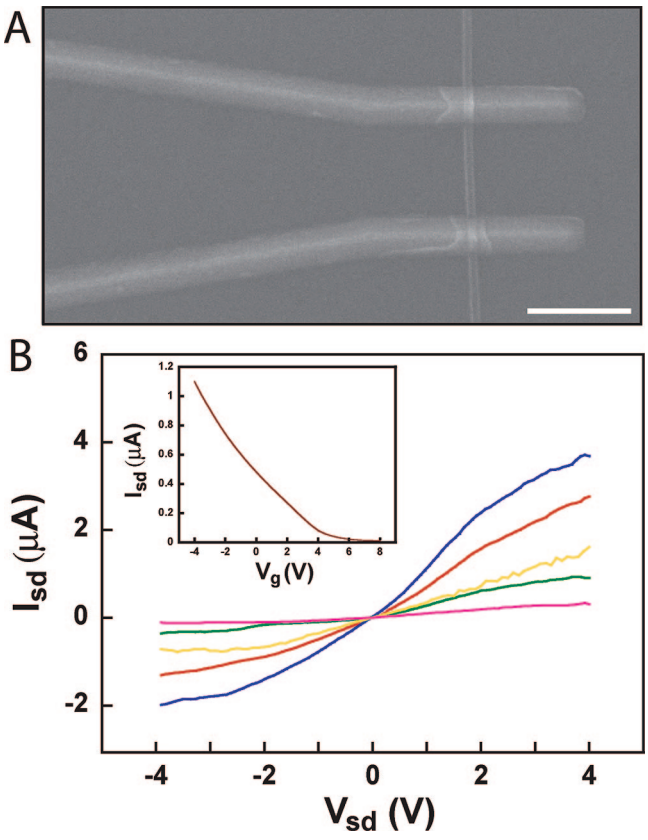

Figure 6. Si nanotube-based FETs. (A) Scanning electron microscopy image of a typical device. Scale bar is 1 μm. (B) Output characteristic of a p-type FET. Current (I) vs voltage (V) recorded on a 20 nm internal-diameter (10 nm wall thickness) boron-doped Si nanotube at various gate voltages (V_g) of: −4 V (pink), −2 V (green), 0 V (yellow), +2 V (red), and −4 V (blue). The inset shows a transconductance curve at V_{sd}= +1 V. Scale bar is 1 μm.

source-drain contacts (typical separation of 1 μm). Next, an annealing step was carried out by rapid thermal annealing (RTA) to form a stable, conducting silicide with a low Schottky barrier. Transport characteristics can then be studied, with the highly doped silicon substrate serving as the back gate. Figure 6B shows the current (I_D) versus drain-source bias (V_D) (output characteristics) of individual p-type silicon-nanotube field-effect transistors at various gate voltages (V_g). This gate-voltage dependence is typical of p-type FETs[43] and is similar to that of nanowire-based FET devices.[24,27,44] This behavior is also shown in the inset, where the current varies with the applied gate voltage (I_{sd}−V_g) at a constant V_{sd} of +1 V.

To summarize, we have synthesized, for the first time, robust, single-crystalline silicon nanotubes from various nanotubular to conical structures, with well-controlled and uniform inner diameters (ranging from 1.5 to 500 nm), wall thickness, taper angle, and chemical composition. The synthesis was carried out with the use of a nanowire-template strategy combined with gold-catalyst-assisted chemical vapor deposition. These findings may lead to novel nanoelectronic, nanophotonic, and nanosensor devices. We have shown that the silicon nanotubes have conventional crystalline silicon structures. Furthermore, these silicon nanotubes were doped in situ with boron and germanium to form p-type silicon nanotubes and SiGe-alloy nanotubes, respectively. This is the first example of in situ-controlled doping of silicon nanotubes. This control over the chemical composition opens up the possibility of achieving high-quality electronic materials and to tune their properties to better suit various applications.

Combined, these strategies have greatly expanded the scope of control over critical parameters of silicon-based nanotubes and thus suggest that our synthesized silicon nanotubular structures are ideal candidates for various biological and chemical applications and nanoscale-device applications. Future work in this area will be application-oriented.

Experimental Section

Growth of Ge−Si Core−Shell Nanowires. Single-crystal Ge−Si core−shell nanowires were synthesized inside a horizontal quartz-tube furnace in the CVD system, with the use of gold nanoclusters (Ted Pella, Inc.) as a catalyst, first deposited on oxidized silicon wafers. Germanium nanowires were grown at 280 °C, from 10% germane in 200 sccm H_2 and 400 torr (axial growth), while the germanium shells for the enlargement process were deposited at 360 °C, at 4 torr (radial growth), at different deposition times. The conical germanium nanowires were grown at higher temperatures (340, 360, and 380 °C) under a flow of germane (30 sccm) and 200 sccm of H_2 at 400 torr for 3 min, to give a cone-like shape, the result of axial and radial growth. Reduction of the above temperatures to 280 °C under continued flow of GeH_4 (30 sccm) leads to funnel-like structures with various taper angles. The temperature was maintained at 280 °C for 20 min, for the purpose of wire growth.

The silicon shells were grown at 450 °C from silane (5 sccm) in a mixture of 5 sccm Ar and 10 sccm H_2 at 1 Torr. Silicon−germanium alloy shells were deposited from silane (0.5 sccm) and 50 sccm of 10% germane in 200 sccm H_2 at 1 torr. The p-type silicon shells were formed by incorporation of diborane (5 sccm) and silane (5 sccm) at 1 torr. Oxidation of the germanium cores to reduce their original diameter was accomplished by flowing oxygen at 1 torr and 250 °C at different oxidation times over a period of 1−3 h.

The substrate-bound Ge−Si core−shell nanowires were then sonicated in pentanol. By subsequent introduction of 1:3 v/v H_2O_2:pentanol at 60 °C for 2−3 h, the as-prepared nanowires were transformed into high-quality single-crystalline silicon nanotubes, without the necessity of thermal annealing. The nanotube samples were centrifuged, washed several times with ethanol, and deposited on oxidized degenerately doped silicon wafer or copper grids or lacey copper grids for electrical transport and TEM measurements, respectively.

Sample Characterization. The structure and composition of the nanostructures were investigated with the use of a 200 kV field-emission-gun transmission electron microscope (Technai F20).

The energy-dispersive X-ray spectra were obtained with an HTEM with a spot size of 2 nm.

TOF-SIMS analysis was conducted by a time-of-flight secondary-ion mass spectrometer (PHI TRIFT II), on a gold-coated silicon wafer containing deposited silicon nanotubes. The Ga^+ primary-ion beam was operated at 25 keV and 20 nA. Positive secondary-ion spectra were acquired from 50 × 50 μm^2 areas of the surfaces. Sputtering was performed by Ga^+ ions for 1 s followed by spectrum acquisition. The sputtering area is 150 × 150 μm^2.

Electrical characterization was carried out by a cryogenic electrical probe station (Janis Inc. model TTP-4).

Nanotubes Surface Modification. All of the modifications were first carried out on the surface of the nanowires. The substrate-bound nanowires were embedded in various solutions of silane derivatives for nearly 2 h to yield both hydrophilic and hydrophobic surfaces: 1% aminosilane and 5% phosphate−silane in water, 2% fluorosilane and 2% octadecylsilane in dichloromethane (CH_2Cl_2). The samples were then rinsed with the appropriate solvent and cured for 10 min at 110 °C. After sonication and etching, the resulting

(43) Patolsky, F.; Zheng, G.; Lieber, C. M. *Nat. Protocols* **2006**, *4*, 1711–1724.
(44) Cui, Y.; Lieber, C. M. *Science* **2001**, *293*, 1289–1292.

functionalized silicon nanotubes were centrifuged, washed, and dispersed into various liquid suspensions (organic solvents and water). The silicon nanotubes obtained possess hydrophilic/hydrophobic exteriors and nonfunctionalized, hydrophilic interiors, which can be readily modified in later steps.

Acknowledgment. We thank Dr. Yossi Lereah for helpful discussions on the analysis of HRTEM experiments. We also thank Dr. Ela Strauss and Dr. Yuri Rosenberg for their help with TOF-SIMS and XRD measurements, respectively. This study was partially supported by the Israel Science Foundation (ISF), Legacy Program, Israel. We thank Mr. Roni Naftali for his generous support.

Supporting Information Available: High-resolution wide-field selected-area diffraction pattern of a representative silicon nanotube, as in Figure 1D red boxed inset, confirming the single-crystalline nature of the obtained tubes (Figure S1); measured interplanar distance and the FFT for Figure 1E, confirming uniform diamond crystal structure of Si (Figure S2A, S2B, and S2C); and lattice-resolved TEM images and their FFT for Figure 1F, showing the uniform crystalline structure of Si (Figure S3A, S3B, and S3C). This material is available free of charge via the Internet at http://pubs.acs.org.

JA808483T